University of Reading

School of Mathematical and Physical Sciences

Computation and Analysis of Baroclinic Rossby Wave Rays in the Atlantic and Paci c Oceans

James Barlow

August 2010

This dissertation is a joint MSc in the Departments of Mathematics and Meteorology and is submitted in partial fulfilment of the requirements for the degree of Master of Science

Contents

List of Figures

Chapter 1

Introduction

Rossby wave theory first came about in 1939 (Rossby, 1939) and suggested the existence of westward propagating signals originating primarily from the eastern boundaries of ocean mode of Rossby wave is a result of the latitudinal variation of phase speed. The phase speed's latitudinal dependence is a result of the β-effect, and is thus often referred to as β-refraction, illustrated by Figure (1.1).

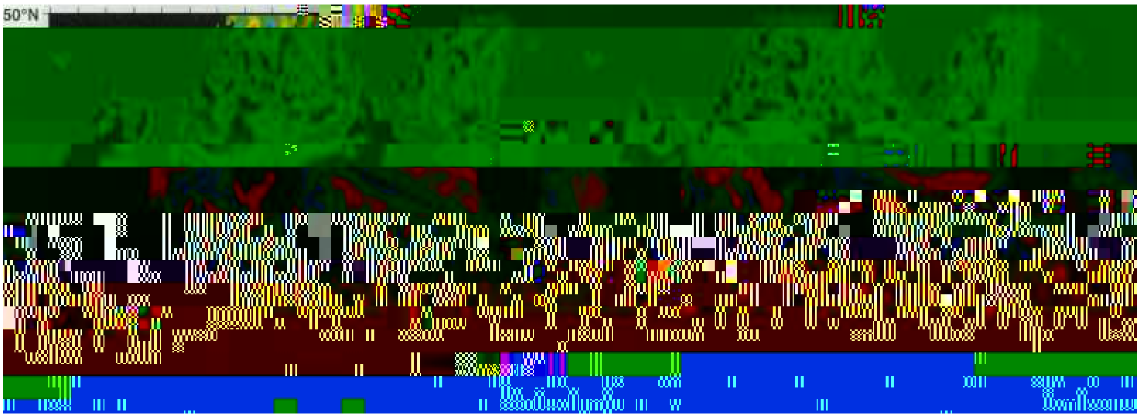

Figure 1.1: White lines identify a westward propagating, β-refracted Rossby wave trough

the interior is dominated by wind stress. Despite this, they also state from their analysis that the e□ects of boundary-driven waves are clear when wind-driven variability is removed from the observational data. This can be seen in Figure (1.2) which illustrates correlation coe□cients in the North Pacific between observed SSH anomali

gravity-wave phase speed is constant, we will introduce an analytical function representative of a more realistic phase speed distribution. This will yield an original result and allow us to examine the effect of a variable phase speed on ray propagation. From the ray solutions, we can gain a visual picture of the potential location of the caustics described in the literature. We will then attempt to locate real coastics in modelled SSH data and compare any results with the theoretical predictions produced from the ray solutions.

1.1 Theory

1.1.1 A Note On WKB Theory

From Equation (1.1) we can therefore write:

$$\frac{\partial}{\partial t}\left[-\left(k_x^2 + k_y^2\right)\Psi - \frac{1}{R^2}\Psi\right] + \beta i k_x \Psi = 0 \qquad (1.4)$$

$$i\omega\left(k_x^2 + k_y^2\right) + \frac{i\omega}{R^2} + \beta i k_x = 0 \qquad (1.5)$$

$$\left[1 + R^2\left(k_x^2 + k_y^2\right)\right]\omega + \beta R^2 k_x = 0 \qquad (1.6)$$

1.1. Ray Equations

Although the phase speed of a Rossby wave is almost always directed purely westward, the group velocity has no such restriction. As the energy associated with Rossby waves propagates with the group velocity c

1.1. Analytical Solution

For the most simple case, an analytical solution can be derived to describe the ray paths. The most simple case relies on a few basic assumptions, that waves are propagating from a straight, north-south orientated eastern boundary, that the gravity-wave phase speed c_0 is constant, and that the phase function S is constant along the eastern boundary. We start by rearranging the dispersion relationship into the following form:

$$\left(k_x + \frac{\beta}{2\omega}\right)^2 + k_y^2 = \frac{\beta^2}{4\omega^2} - \frac{f^2}{c_0^2} \tag{1.27}$$

Under the assumption that the wave amplitude is slowly varying compared to variations in the phase, it is possible to use WKB ideas. We therefore refer back to and redefine equations (1.10) and (1.11), which under WKB theory mean that the locally defined wavenumbers must satisfy the dispersion relationship ω:

$$\begin{aligned} k_x &= \frac{\partial S}{\partial x} \\ k_y &= \frac{\partial S}{\partial y} \end{aligned} \tag{1.28}$$

From equation (1.28), an added constraint is that the wavenumbers must also satisfy the following compatibility condition:

$$\frac{\partial k_x}{\partial y} = \frac{\partial k_y}{\partial x} \tag{1.29}$$

If we consider Rossby waves of a constant frequency, we need only solve equations for the wavenumbers k_x and k_y and not ω. Differentiating equation (1.27) with respect to x yields:

$$2k_x\frac{\partial k_x}{\partial x} + \frac{\beta}{\omega}\frac{\partial k_x}{\partial x} + 2k_y\frac{\partial k_y}{\partial x} = 0 \tag{1.30}$$

This is equivalent to:

$$\left(k_x + \frac{\beta}{2\omega}\right)\frac{\partial k_x}{\partial x} + k_y\frac{\partial k_y}{\partial x} = 0 \tag{1.31}$$

Using the compatibility condition specified by equation (1.29), this can be written as follows:

$$\left(k_x + \frac{\beta}{2\omega}\right)\frac{\partial k_x}{\partial x} + k_y\frac{\partial k_x}{\partial y} = 0 \tag{1.32}$$

This equation takes on the form of a quasi-linear first order partial differential equation:

$$a(x,y,k_x)\frac{\partial k_x}{\partial x} + b(x,y,k_x)\frac{\partial k_x}{\partial y} = c(x,y,k_x) \tag{1.33}$$

where

$$\begin{aligned} a &= k_x + \frac{\beta}{2\omega} \\ b &= k_y \\ c &= 0 \end{aligned} \tag{1.34}$$

We define the ray trajectory for which we want to solve as the curve $r\,(x(t), y(t), k_x(t))$ which must satisfy:

$$\frac{dr}{dt} = (a, b, c) \tag{1.35}$$

It is clear that equation (1.35) represents a system of differential equations that describes the path of group velocity and variations in the zonal and meridional wavenumbers of the Rossby waves:

$$\frac{dx}{dt} = k_x + \frac{\beta}{2\omega} \tag{1.36}$$

$$\frac{dy}{dt} = k_y \tag{1.37}$$

$$\frac{dk_x}{dt} = 0 \tag{1.38}$$

$$\frac{dk_y}{dt} = -\frac{\beta f}{c_0^2} \tag{1.39}$$

The equation for the ray trajectory is therefore given by:

$$\frac{dy}{dx} = \frac{k_y}{k_x + \beta/(2\omega)} \tag{1.40}$$

As we have assumed a constant frequency, $\omega = \omega_0$ and clearly from equation (1.38), $k_x = k_{x0}$ remains constant along each ray. The remaining solutions to the ray equations, as derived by Grimshaw and Allen (1983), are given as follows:

$$x = x_0 + \left(k_x + \frac{\beta}{2\omega}\right)t \tag{1.41}$$

$$y = y_0 \cos\left(\frac{\beta t}{c_0}\right) \tag{1.42}$$

$$k_y = -\frac{\beta y_0}{c_0} \sin\left(\frac{\beta t}{c_0}\right) \tag{1.43}$$

where x_0 and y_0 are the coordinates of the starting point of the ray trajectory. Using the equations for x and y, a constant gravity-wave phase speed of $c_0 = 3ms^{-1}$ and specifying ω such that it corresponds to semi-annual frequency Rossby waves, we can immediately reproduce the solution derived by Schopf et al. (1981) propagating from a straight north-south orientated boundary. This is illustrated by Figure (1

latitude, where for example $y = 1000\text{km}$ or $y = -1000\text{km}$ represents a position 1000km north or south of the equator respectively. Under the β-approximation, we make the assumption that the β-parameter is constant, and thus that the Coriolis parameter $f = \beta y$ varies linearly with latitude. We approximate β with:

$$\beta \quad \frac{2\Omega}{a} \quad 2.288 \times 10$$

The autonomous system is derived as follows. We know from equ in which case we take as a boundary condition that the phase, S is constant along the boundary. In this case it can be shown that:

$$\frac{\partial S}{\partial y} = k_y = 0 \tag{2.15}$$

The meridional wavenumber k_y will therefore have a zero initial value for each ray trajectory. This assumption is valid only while the coastline is straight and has a north-south orientation, but not in the more general case of a variable coastline. The initial value of x solutions is known as the caustic line which we will discuss in more detail later. Important to note is the symmetry of the solution about the equator.

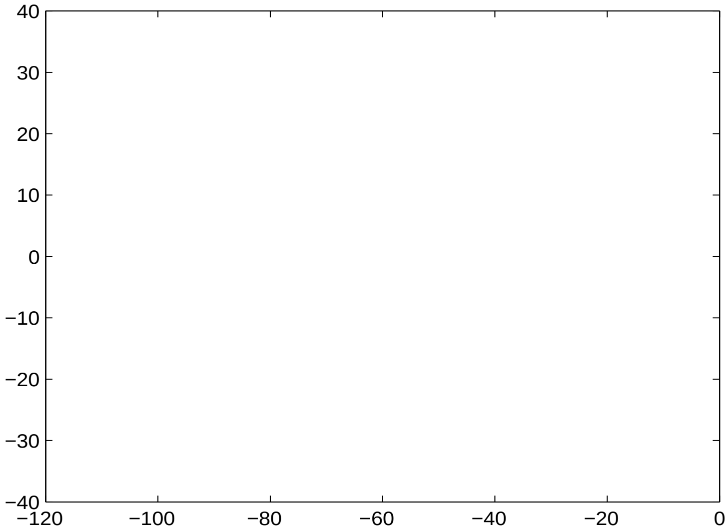
40
30
20
10
0
−10
−20
−30
−40
−120
−100
−80
−60
−40
−20
0

$$y_c = \frac{c_0}{2\omega} \tag{2.24}$$

10250km from the eastern boundary, a result consistent with the graphical representation given in Figure (2.3). The location of this energy focus is expected to be an area of very intense Rossby wave activity.

.1. Realistic Coastlines

Thus far we have only considered wave propagation from a straight, north-south bound-

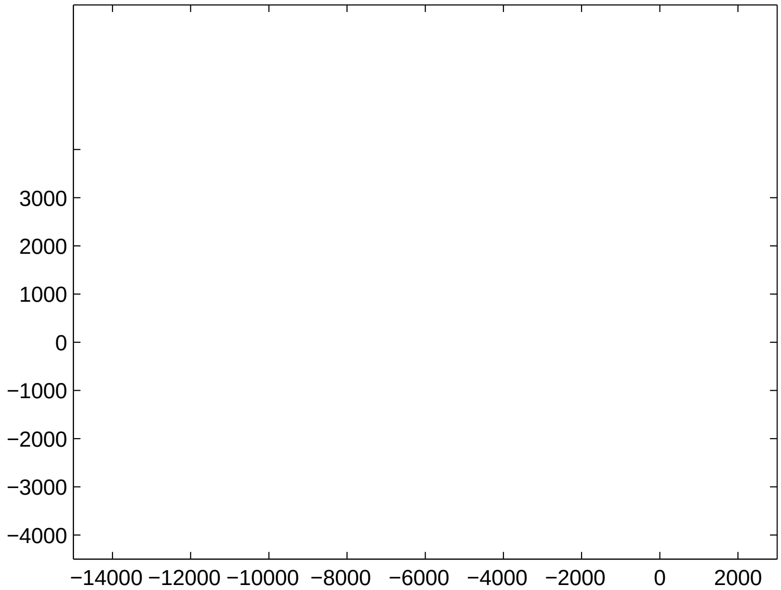
3000
2000
1000
0
−1000
−2000
−3000
−4000
−14000 −12000 −10000 −8000 −6000 −4000 −2000 0 2000

introducing a variable meridional wavenumber along the boundary is that the ray paths are now initially orientated slightly towards the south as they leave the coastline. In addition, the angle of the boundary means that the caustic in

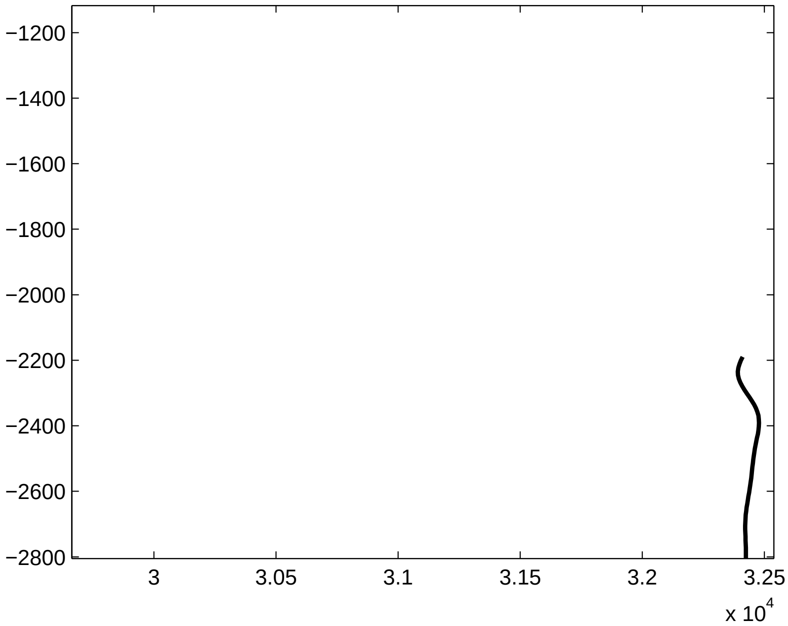
−1200
−1400
−1600
−1800
−2000
−2200
−2400
−2600
−2800
3
3.05
3.1
3.15
3.2
3.25
x 10^4

$$c_0(x,y) = A + B\cos\left(\frac{2y}{a}\right) + C\cos\left(\frac{6y}{a} + D\pi\right) + \frac{Ex}{a}; \qquad (2.39)$$

where the additional parameter E

distribution of c_0

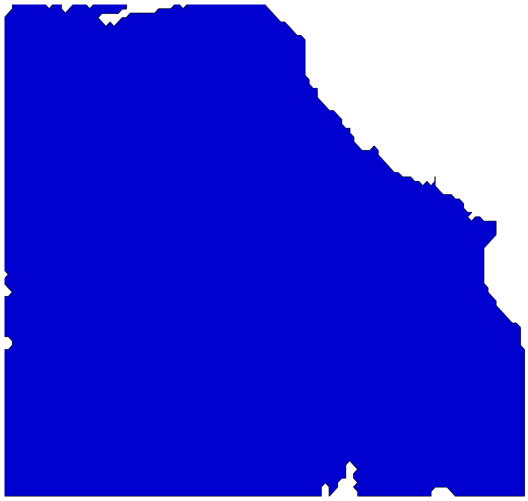

$$\frac{d\varphi}{dt} = c_{g\varphi} = \frac{\partial\omega}{\partial k_\varphi} = \frac{2\beta R\ a\cos^3\varphi k_\lambda k_\varphi}{\left[a^2\cos^2\varphi + R^2\left(k_\lambda^2 + \cos^2\varphi k_\varphi^2\right)\right]^2} \tag{2.47}$$

$$\frac{dk_\lambda}{dt} = -\frac{\partial\omega}{\partial\lambda} = 0 \tag{2.48}$$

$$\frac{dk_\varphi}{dt} = -\frac{\partial\omega}{\partial\varphi} = -\frac{2\beta R^2 a k_\lambda\left(R^2\sin^2\varphi k_\lambda^2 + a^2\cos\ \varphi\right)}{\sin\varphi\left[a^2\cos^2\varphi + R^2\left(k_\lambda^2 + \cos^2\varphi k_\varphi^2\right)\right]^2} \tag{2.49}$$

It can once more be shown from equation (2.46) that in order for the group velocity to be negative in the λ-direction, the following condition must be satisfiJΩ/R1310.90913542211.8413(o)28.0953(v

Thus our autonomous system of differential equations is given as:

$$\frac{d\varphi}{d\lambda} = \frac{-2R^2 k_\lambda k_\varphi}{\left[a^2 + R^2\left(k_\varphi^2 - k_\lambda^2/\cos^2\varphi\right)\right]} \tag{2.56}$$

$$\frac{dk_\lambda}{d\lambda} = 0 \tag{2.57}$$

$$\frac{dk_\varphi}{d\lambda} = \frac{2k_\lambda\left(R^2\sin^2\varphi k_\lambda^2 + a^2\cos\ \varphi\right)}{\sin\varphi\cos^3\varphi\left[a^2 + R^2\left(k_\varphi^2 - k_\lambda^2/\cos^2\varphi\right)\right]} \tag{2.58}$$

. . Fixed ω Solution

From this we can calculate the maximum frequency for which Rossby waves can propagate use a conversion ratio of 112km per degree, then the critical latitude for the cartesian coordinate solution in degrees is approximately 58.3°. It is therefore clear that converting

Variable Meridional Wavenumber

. . Variable c_0

The last step to achieve the final result in spherical polar coordinates is to remove the assumption that the gravity-wave phase speed is constant. Rather than using $c_0 = 2.6\mathrm{ms}^{-1}$, we will once more use the phase speed function specified by equation (2.37). In spherical polar coordinates this is equivalent to:

$$c_0(\varphi) = A + B\cos(2\varphi + C\pi) + D\cos(6\varphi + \pi)\,; \tag{2.74}$$

since $\varphi = y/a$. Re-deriving the ray equations becomes a little more tedious due to the additional φ dependent terms, but the general autonomous form of the equation for k_φ can be written:

$$\frac{dk_\varphi}{d\lambda} = \frac{1}{c_{g\lambda}}\left[\frac{\partial\omega}{\partial R^2}\frac{\partial R^2}{\partial\varphi} + \frac{\partial\omega}{\partial\beta}\frac{\partial\beta}{\partial\varphi} + \frac{\partial\omega}{\partial k_x}\frac{\partial k_x}{\partial\varphi}\right] \tag{2.75}$$

where $R = c_0(\varphi)/2\Omega\sin\varphi$ and $k_x = k_\lambda/a) =$

. Caustics

In comparing the final results in cartesian coordinates and spherical polar coordinates (shown by Figures (2.14) and (2.18) respectively), it can be seen that there is very little

in red. In addition we include the western coastlines to give a better overall picture.

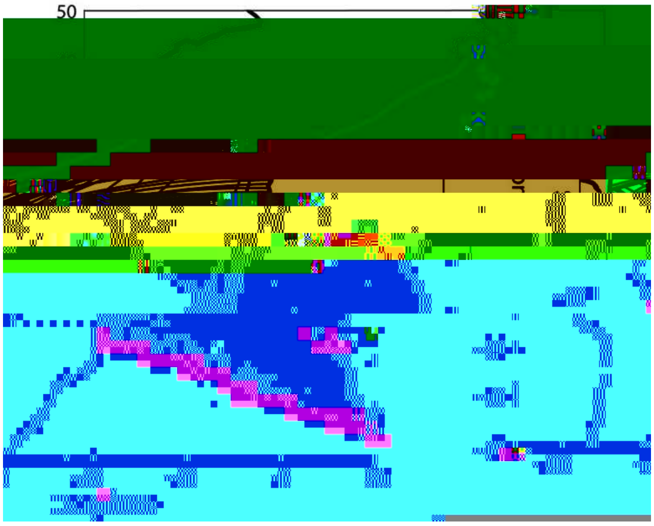

Figure 2.19: Caustics in the Atlantic Ocean

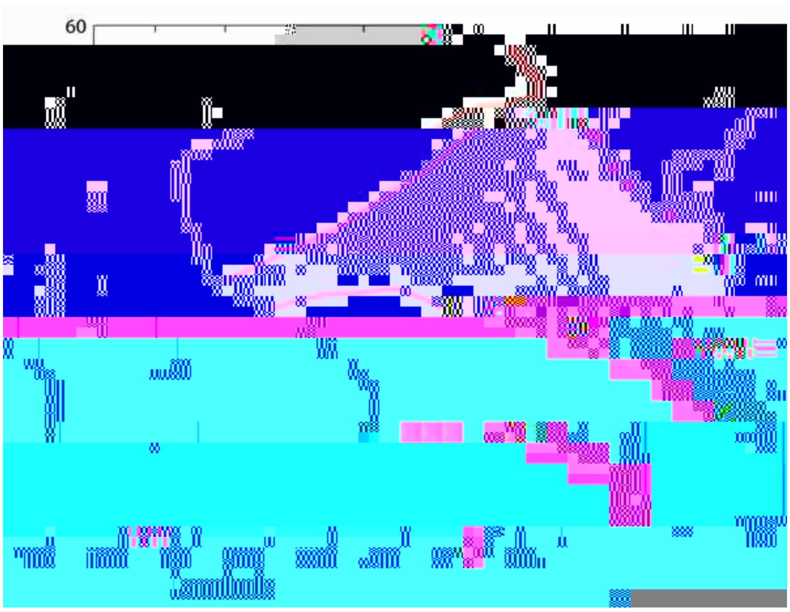

Figure 2.20: Caustics in the Pacific Ocean

For the Atlantic Ocean, the model solution suggests that the critical latitude in the Northern Hemisphere is at approximately φ_c 40°N on the eastern coastline. In the Southern Hemisphere the critical latitude is at the southern tip of Africa at φ_c 35°S where the coastline comes to an end. The poleward extent of the caustic decreases almost linearly westwards (towards the equator) in both hemispheres, until the western coastline is reached. The focus of rays that we have seen in solutions with the western coastline hidden does not occur in the Atlantic because the ocean basin is not wide enough. The caustics instead meet the western coastline at 13°

Chapter

Analysis of Model Output

Many recent studies have used either satellite altimeter da

example of an unfiltered and filtered time series is given by Figure (3.1), below. Finally,

Computational restraints meant that in the current study, w

Chapter

Conclusions and Further Work

.1 Summary

During this project we have modelled ray propagation in the Atlantic and Pacific ocean basins both in cartesian and spherical polar coordinates. We began by considering a straight eastern boundary, both north-south orientated and orientated at some angle α. We then extended the ideas to account for variable coastline geometry and introduced eastern boundaries representative of the Atlantic and Pacific coastlines.

Introducing a variable coastline required us to introduce a new boundary condition dependent on the angle of the coastline α. The boundary condition was used to determine the initial values of the zonal and meridional wavenumbers. Having introduced the new boundary condition, it was found that trapped waves in regions equatorwards of the critical latitude φ_c were unable to propagate freely as Rossby waves if α is sufficiently large. This indicates that Rossby waves are not able to propagate from all regions equatorwards of φ_c. Variable coastal geometry also creates differences in the initial tilting of the rays as they propagate away from the boundary, and this leads to the divergence and convergence of rays in some regions. The shape of the coastline therefore has significant impacts on the energy distribution of the boundary-driven waves throughout the ocean basin. This observation may be related to the pattern of correlation coefficients shown in Figure (1.2) from Fu and Qiu (2002) and as discussed in Chapter (2.3).

also determines whether Rossby waves can propagate freely from regions equatorwards of φ_c if α is also significant. As the Rossby radius of deformation R is dependent on c_0 and we determined that the latitudinal variation in R was significant for shaping the ray envelope, we deduced that c_0 is also an important variable in determining the location of the caustics.

The solutions derived in cartesian coordinates and spherical coordinates were found to be very similar, indicating that the shape of the ray envelope is not strongly dependent on the sphericity of the Earth.

Having produced some graphical representation of the ray propagation patterns across each ocean basin, we briefly discussed the presence of the caustics. The caustics are theoretical lines that meet the eastern boundary at the critical latitude and North of which we expect waves at the boundary to remain trapped as coastally-trapped Kelvin waves. Equatorwards of the critical latitude, provided that the coastline angle is not sufficiently large, waves can propagate freely from the coast as Rossby waves. In the interior ocean, the caustics define the western extent of the region where we expect to find a significant amount of variability associated with boundary driven waves. Westward of the caustic, variability associated with the boundary driven waves is expected to decay exponentially. The pattern of real ray solutions within the caustic region indicated that rays propagating from the eastern boundary turned and headed equatorwards. As a ray trajectory represents the group velocity vector, and energy associated with boundary driven Rossby waves propagates with the group velocity, the theory therefore indicates that energy from the mid-latitudes propagates equatorwards via dispersion, as opposed to the western part of this region latnpagen2748(s)0.08958(d)0.328980492351(u)0.380099(n)0.0739751(k)0.234986239.488(l)-0.248(

the contours and the modelled caustic. This is a good early indicator that dispersion is

The next step to improve the model is therefore to include some steps to compute the point at which each ray trajectory first crosses with another. The line that passes through each of these points is the caustic.

We previously stated that a caustic appears when two neighbo

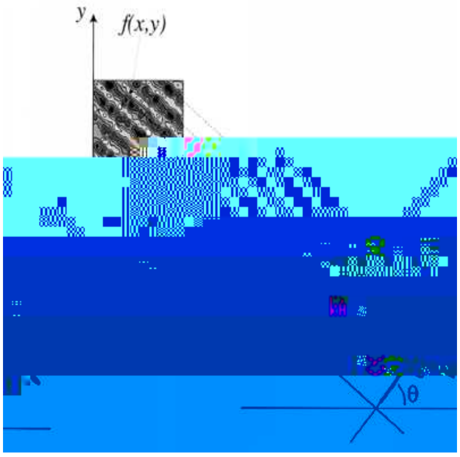

Figure 4.1: Challenor et al. (2001)

As we have seen, westward propagating signals in ocean data can best be illustrated by arranging data into a Hovmöller diagram. Zonally-propagating features subsequently appear as slanted propagation patterns where the angle at which the feature slants is determined by its phase speed. Having applied the Radon Transform to a Hovmöller diagram, we would therefore expect a maxima to occur in θ when x′ is perpendicular to the sloping features that represent the westward propagating signals. By determining the maxima and minima associated with certain angles within the time-longitude plot, we can thus identify signals that are purely westward propagating. Then by applying a Gaussian filter, as in Huntin Hu.900.625(a)-4004-0.2402.041-16.434TdΩJΩ-272.010TdΩ[(p)0.3()0.32898(g)609359r

Chapter

Appendix 1

.1 Variabl

(5.59

$$r_3 = \frac{4AB\cos\varphi 2}{d_1} \tag{5.9}$$

$$r = \frac{12AD\sin\varphi_1}{d_2} \tag{5.10}$$

$$r = \frac{4AD\cos\varphi_1}{d_1} \tag{5.11}$$

$$r = \frac{4B^2\cos\varphi_2\sin\varphi_2}{d_2} \tag{5.12}$$

$$r = \frac{2B^2\cos^2\varphi_2}{d_1} \tag{5.13}$$

4B Dc φ 2

$$r = \frac{4BD\cos\varphi_2\cos\varphi_1}{d_2} \tag{5.14}$$

$$(f^2)_\varphi = 8\Omega^2 \cos\varphi \sin\varphi \tag{5.23}$$

The following equations are the terms of the resulting derivative of R^2:

$$q_1 = \frac{A^2 (f^2)_\varphi}{f} \tag{5.24}$$

$$q_2 = \frac{4AB\sin\varphi_2}{f^2} \tag{5.25}$$

$$q_3 = \frac{2AB\cos\varphi_2 (f^2)_\varphi}{f} \tag{5.26}$$

$$q \;\; = \frac{12AD\sin\varphi_1}{f^2} \tag{5.27}$$

$$q \;\; = \frac{2AD\cos\varphi_1 (f^2)_\varphi}{f} \tag{5.28}$$

$$q \;\; = \frac{12BD\sin\varphi_1 \cos\varphi_2}{f^2} \tag{5.29}$$

$$q \;\; = \frac{4BD\cos\varphi_1 \sin\varphi_2}{f^2} \tag{5.30}$$

$$q \;\; = \frac{2BD\cos\varphi_1 \cos\varphi_2 (f^2)_\varphi}{f} \tag{5.31}$$

$$q \;\; = \frac{8B^2 \cos\varphi_2 \sin\varphi_2}{f^2} \tag{5.32}$$

$$q_{10} = \frac{B^2 \cos^2\varphi_2 (f^2)_\varphi}{f} \tag{5.33}$$

$$q_{11} = \frac{12D^2 \cos\varphi_1 \sin\varphi_1}{f^2} \tag{5.34}$$

$$q_{12} = \frac{D^2 \cos^2\varphi_1 (f^2)_\varphi}{f} \tag{5.35}$$

Therefore the derivative of R^2 is:

$$(R^2)_\varphi = \sum_{i=1}^{12} q_i \tag{5.36}$$

The equation for k_φ becomes:

$$\frac{dk_\varphi}{d\lambda} = \frac{\left((R^2)_\varphi a^2 \cos^3\varphi - 2R \;\; \sin\varphi k_\lambda^2\right) k_\lambda}{R \;\; \cos^3\varphi \left[a^2 + R^2 \left(k^2\right.\right.}$$

Chapter

References

Challenor, P. G., Cipollini P., Cromwell D., 2001, Use of the 3D Radon Transform to Examine the Properties of Oceanic Rossby Waves, J. Atmos. Ocn. Tech., 18, 1558-1566

Chelton D. B., Schlax M. G., 1996, Global Observations of Oceanic Rossby Waves, Science, 272, 234-238

Chelton D. B., DeSzoeke R. A., Schlax M. G., Naggar K., Siwertz N., 1998, Geographical Variability of the First Baroclinic Rossby Radius of Deformation, J. Phys. Oceanogr., 28, 433-460

Fu L.-L., Qiu B., 2002, Low-frequency variability of the North Pacific Ocean: The roles of boundary- and wind-driven baroclinic Rossby waves, J. Geophys. Res, 107(C12), 3220, doi:10.1029/2001JC001131

Grimshaw R., Allen J. S., 1983, Low-Frequency Baroclinic Waves off Coastal Boundaries, J. Phys. Oceanogr., 18, 1124-1142

Hunt F., 2009, The Vertical Structure of Oceanic Rossby Waves, University of Reading MSc Dissertation

Killworth, P. D., Chelton D. B., de Szoeke R. A., 1997, The speed of observed and theoretical long extratropical planetary waves, J. Phys. Oceanogr., 27, 19461966

Killworth P. D., Blundell J. R., 1999, The Effect of Bottom Topography on the Speed of Long Extratropical Planetary Waves, J. Phys. Oceanogr., 29, 2689-2710

Killworth P. D., Blundell J. R., 2003, The Dispersion Relati